Missouri State University

BearWorks

College of Health and Human Services

2012

Biomolecular Triconjugates Formed between Gold, Protamine, and Nucleic Acid: Comparative Characterization on the Nanoscale

Robert DeLong
Missouri State University

Lisa Cillessen
MSU Undergraduate

Chris Reynolds
MSU Undergraduate

Adam Wanekaya
MSU Undergraduate

Tiffany Severs
MSU Graduate Student

See next page for additional authors

Follow this and additional works at: https://bearworks.missouristate.edu/articles-chhs

Recommended Citation

DeLong, Robert K., Lisa Cillessen, Chris Reynolds, Adam Wanekaya, Tiffany Severs, Kartik Ghosh, Michael Fisher et al. "Biomolecular triconjugates formed between gold, protamine, and nucleic acid: comparative characterization on the nanoscale." Journal of Nanotechnology (2012).

This article or document was made available through BearWorks, the institutional repository of Missouri State University. The work contained in it may be protected by copyright and require permission of the copyright holder for reuse or redistribution.
For more information, please contact BearWorks@library.missouristate.edu.

Authors

Robert DeLong; Lisa Cillessen; Chris Reynolds; Adam Wanekaya; Tiffany Severs; Kartik Ghosh; Michael Fisher; Stephanie Barber; John Black; and For complete list of authors, see publisher's website.

This article is available at BearWorks: https://bearworks.missouristate.edu/articles-chhs/289

Hindawi Publishing Corporation
Journal of Nanotechnology
Volume 2012, Article ID 954601, 9 pages
doi:10.1155/2012/954601

Research Article

Biomolecular Triconjugates Formed between Gold, Protamine, and Nucleic Acid: Comparative Characterization on the Nanoscale

Robert K. DeLong,[1] Lisa Cillessen,[2] Chris Reynolds,[3] Adam Wanekaya,[3] Tiffany Severs,[3] Kartik Ghosh,[4] Michael Fisher,[5] Stephanie Barber,[6] John Black,[7] Ashley Schaeffer,[1] and Kristin J. Flores[1]

[1] *Cell and Molecular Biology Program, Department of Biomedical Sciences, Missouri State University, Springfield, MO 65897, USA*
[2] *College of Pharmacy, The Ohio State University, Columbus, OH 43210, USA*
[3] *Department of Chemistry, Missouri State University, Springfield, MO 65897, USA*
[4] *Department of Physics Astronomy and Materials Science, Missouri State University, Springfield, MO 65897, USA*
[5] *School of Medicine, University of North Carolina at Chapel Hill, Chapel Hill, NC 27599, USA*
[6] *George Warren Brown School of Social Work, Washington University in St. Louis, St. Louis, MO 63130, USA*
[7] *School of Medicine, University of Pittsburgh, Pittsburg, PA 15261, USA*

Correspondence should be addressed to Robert K. DeLong, robertdelong@missouristate.edu

Received 15 June 2011; Accepted 11 August 2011

Academic Editor: Dongwoo Khang

Copyright © 2012 Robert K. DeLong et al. This is an open access article distributed under the Creative Commons Attribution License, which permits unrestricted use, distribution, and reproduction in any medium, provided the original work is properly cited.

DNA and RNA micro- and nanoparticles are increasingly being used for gene and siRNA drug delivery and a variety of other applications in bionanotechnology. On the nanoscale, these entities represent unique challenges from a physicochemical characterization perspective. Here, nucleic acid conjugates with protamine and gold nanoparticles (GNP) were characterized comparatively in the nanorange of concentration by UV/Vis NanoDrop spectroscopy, fluorimetry, and gel electrophoresis. Given the intense interest in splice-site switching oligomers (SSOs), we utilized a human tumor cell culture system (HeLa pLuc-705), in which SSO-directed splicing repair upregulates luciferase expression, in order to investigate bioactivity of the bionanoconjugates. Process parameters important for bioactivity were investigated, and the bimolecular nanoconjugates were confirmed by shifts in the dynamic laser light scatter (DLLS), UV/Vis spectrum, gel electrophoresis, or sedimentation pattern. The data presented herein may be useful in the future development of pharmaceutical and biotechnology formulations, processes, and analyses concerning protein, DNA, or RNA bionanoconjugates.

1. Introduction

Nanoparticles bearing siRNA have been tested recently in clinical trials [1]. RNA oligonucleotides known as splice-shifting oligomers (SSOs) have the ability to correct errors that occur in gene splicing at the RNA level, potentially a novel means of controlling an important molecular pathology underlying cancer [2] and possibly other human diseases [3]. Although protamine has long been known to bind and condense DNA into nanoparticles [4] active for gene delivery [5], condensation of RNA is more controversial [6, 7]. Considering the well-known cell-penetrating and nuclear localization capabilities of protamine [8], we presume it could play a critical role for the delivery of SSOs [9].

To investigate the bioactivity and biocompatibility of the conjugates in this study, we utilize the well-described HeLa pLuc-705 cell culture system, in which luciferase is upregulated by delivery of specific SSOs [10–12]. This luminescence-based assay can be used for quantifying RNA nanoconjugate delivery. We use this system, along with high-throughput screening, to explore the process parameters that are important for the RNA nanoconjugate SSO

bioactivity. To demonstrate the biocompatibility of the triconjugates, we use the MTT (3-(4,5-dimethylthiazol-2-yl)-2,5-diphenyltetrazolium bromide) assay to investigate the metabolic activity of the HeLa pLuc-705 cell line, after incubation with the conjugates. Recently, we reported detection of RNA nanoparticles after protamine complexation to RNA by dynamic laser light scatter spectroscopy (DLLS) [9]. Moreover, gold nanoparticles (GNPs) are taken up by HeLa cells [13], and surface modification of GNPs has been shown to affect their interaction at the plasma membrane and intracellular activity [14]. In this study we characterize conjugates of GNP, with protamine and RNA, in comparative analyses using luminometery, UV/Vis spectroscopy, fluorescence, and gel electrophoresis assays.

2. Experimental

2.1. GNP, Protamine, and Other Reagents. GNPs with a uniform size of ~20–30 nm were synthesized using the standard method of citrate reduction of $HAuCl_4$ salt. Hydrogen tetrachloroaurate (III) trihydrate ($HAuCl_4 \cdot 3H_2O$) was obtained from Fisher Scientific (Fair Lawn, NJ). Sodium citrate was obtained from Spectrum Chemical Corp. (New Brunswick, NJ). To produce the GNPs, an aqueous solution of $HAuCl_4$ (1 mM, 500 mL) was brought to reflux while stirring, and 50 mL of 38.8 mM trisodium citrate solution was rapidly added. After 15 min, the preparation was allowed to cool to room temperature and subsequently filtered through a 0.45 μm filter.

Plasmid DNA encoding Hepatitis B DNA vaccine was obtained as previously described [9]. In some cases, lambda phage DNA (Sigma-Aldrich) was used in the spectral and conjugate studies. The protamine stock was purchased from Sigma-Aldrich as Grade III protamine sulfate salt, derived from herring. Ribonucleic acid (RNA) diethylaminoethanol salt Type IX was also purchased from Sigma-Aldrich and dissolved in RNase-free water just prior to use. A protamine : H_2O standard curve was prepared by dissolving protamine in water at 2 mg/mL, then performing serial dilutions to produce 1 mg/mL, 0.5 mg/mL, 0.25 mg/mL, 0.125 mg/mL, and 0.0625 mg/mL solutions. An RNA : H_2O standard curve was prepared similarly by dissolving RNA in water at 2 mg/mL, then performing serial dilutions to produce 1 mg/mL, 0.5 mg/mL, 0.25 mg/mL, 0.125 mg/mL, and 0.0625 mg/mL solutions.

2.2. High-Throughput Experimental Design to Analyze the Parameters That Affect Bioactivity. Using the HeLa pLuc-705 model, a high-low experimental design was combined with multiparameter screening with a measurable biological activity outcome: relative luminescence (RLU) due to the SSO delivery. The parameters tested included number of cells, time of transfection, mixation rate, and protamine, SSO, magnesium, and ethanol concentration, as illustrated in Figure 2.

2.3. Dynamic Laser Light Scatter Spectroscopy (DLLS). DLLS was conducted on a Malvern Zetasizer Nano-ZS90. Samples were analyzed in 1 mL double-distilled deionized water in UV-transparent Sarstedt cuvettes. Briefly, 1 mg/mL protamine was added to DNA at 0.1 mg/mL while vortexing for 5–10 sec and/or to approximately 50 microlitres of GNPs (3×10^{-8} M). The conjugates were then analyzed directly by DLLS or UV/Vis spectroscopy.

2.4. Fluorimetric and NanoDrop UV/Vis Spectroscopy. Fluorimetric and NanoDrop UV/Vis spectroscopy was conducted as described previously [9] for the Hoechst assay, and the PicoGreen assay was performed in parallel following manufacturer's recommendations. RNA stock solutions were prepared with RNase-free H_2O. Experiments were executed in triplicate, and indicated by Samples A, B, and C for each graph. Serial dilution was performed with 250 μL of solution with 250 μL of RNase free H_2O. Absorbance spectral scans were performed from 190 to 300 nm on a Thermo Fisher NanoDrop 2000c. The UV/Vis absorption spectrum for RNA was also performed in triplicate for 100 ng/μL along with its serial dilution and standard curve for the absorbance values (ordinate) versus concentration (abscissa). For the spectral shift experiments, 90 μL of GNP stock solution was added to 5 μL (10 mg/mL) RNA solution, 5 μL RNase free water, the suspension was vortexed incubated at room temperature for 15 to 20 mins mixed and read on the NanoDrop directly. For GNP-Protamine, 90 μL GNP stock solution and 5 μL (2 mg/mL) stock protamine solution, 5 μL RNase free water was mixed and read as above. For the GNP-protamine : RNA, 90 μL GNP stock solution and 5 μL (10 mg/mL) RNA solution with 5 μL (2 mg/mL) stock protamine solution was mixed and read as above.

2.5. Gel Electrophoresis. Gel electrophoresis was accomplished as described previously [9]. Briefly, the gels contained 2% mass/volume agarose in 1X (v/v) TAE buffer. Each RNA sample contained ethidium bromide (Sigma-Aldrich, St. Louis, MO) at a final concentration of approximately 0.1 mg/mL. Samples contained equal volumes of bromophenol blue loading dye and 5 mg/mL RNA solution. RNA gels were run at 60 V visualized on a Gel Logic imaging station.

2.6. Sedimentation Coupled to UV/Vis NanoDrop. For the sedimentation analysis by UV/Vis NanoDrop, all samples were prepared in triplicate, from the following stock solutions: 200 μL aliquot of the GNP solution, 200 μL of 1.0 mg/mL protamine solution, and 200 μL 5.0 mg/mL RNA solution.

For the GNP only sample, 20 μL of GNP stock solution was added to each microcentrifuge tube. The absorbance from each sample was read, in triplicate, at 525 nm, using the NanoDrop 2000. The samples were centrifuged for 7 minutes at 15,000 rpm, at 10°C. An absorbance reading of the supernatant was taken immediately, at 525 nm.

For the GNP : protamine sample, 20 μL of GNP stock solution was added to each microcentrifuge tube, followed by the addition of 20 μL of protamine stock solution. The samples were vortexed for 8 seconds, and allowed to incubate at room temperature for 5 minutes. The absorbance was

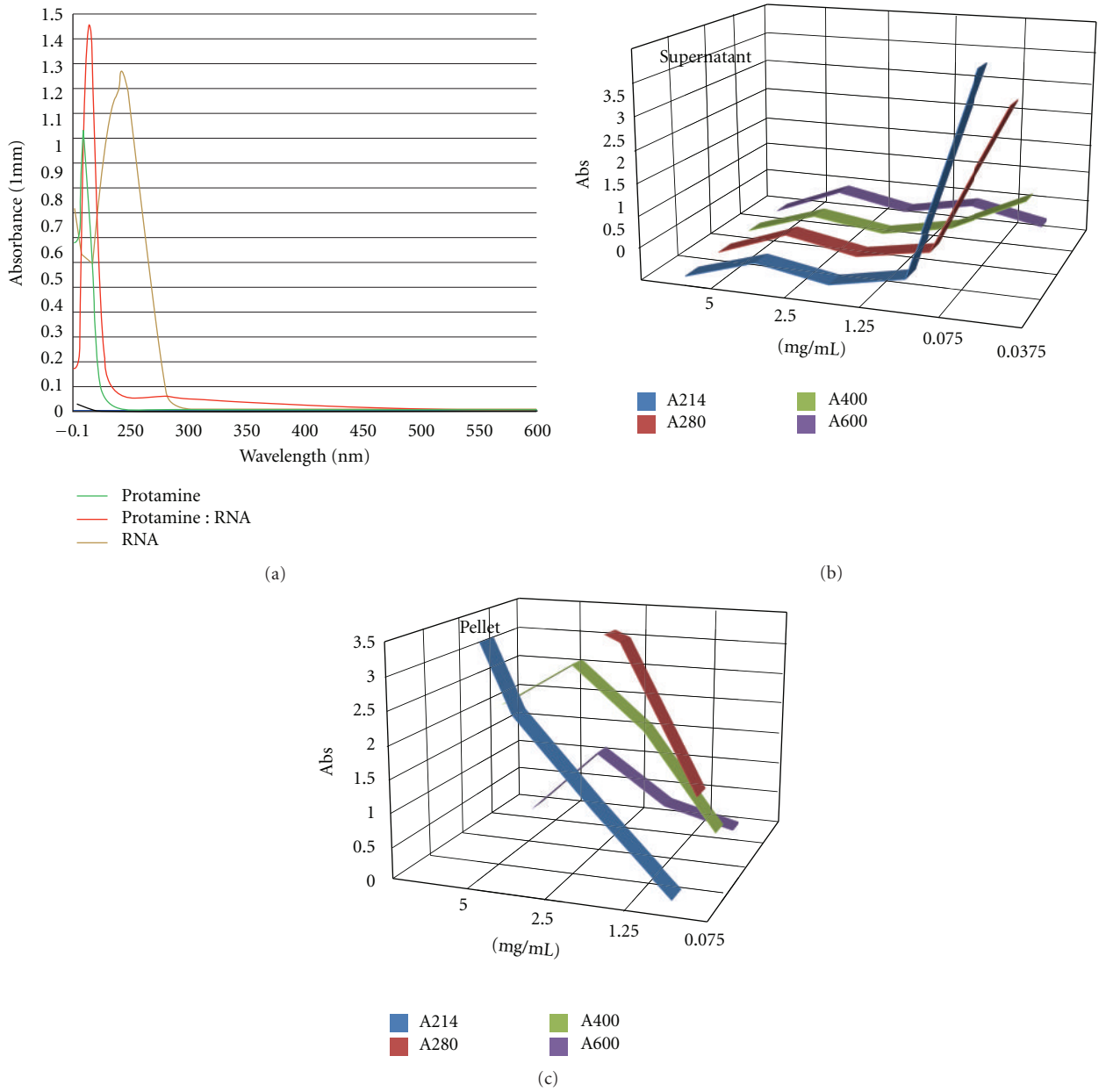

Figure 1: NanoDrop UV/Vis analysis of protamine : RNA and analysis of the sedimentation profiles at 214, 280, 400, and 600 nm.

read; the samples were centrifuged, followed by another absorbance reading of the supernatant, as stated above.

For the GNP : RNA sample, 20 μL of GNP stock solution was added to each microcentrifuge tube, followed by the addition of 20 μL of RNA stock solution. The samples were vortexed for 8 seconds, and allowed to incubate at room temperature for 5 minutes. The absorbance was read at 260 nm. After the samples were centrifuged for 7 minutes at 15,000 rpm, at 10°C, an absorbance reading of the supernatant was taken at 260 nm.

For the sedimentation analysis of the triconjugates, 20 μL of GNP stock solution was added to each microcentrifuge tube, followed by the addition of 20 μL of protamine stock solution, and 20 μL of the RNA stock solution. The samples were vortexed for 8 seconds, and allowed to incubate at room temperature for 5 minutes. The absorbance was read at 260 nm; the samples were centrifuged, followed by another absorbance reading of the supernatant, at 260 nm.

2.7. MTT Assay to Quantify Metabolic Activity after Incubation with Conjugates. Metabolic activity of the HeLa pLuc-705 cells was assessed by the reduction of the yellow tetrazolium salt MTT (3-(4, 5-dimethylthiazol-2-yl)-2,5-diphenyltetrazoliumbromide) to purple, insoluble formazan. All cell culture work was performed under the laminar flow hood, using sterile technique. The HeLa pLuc-705

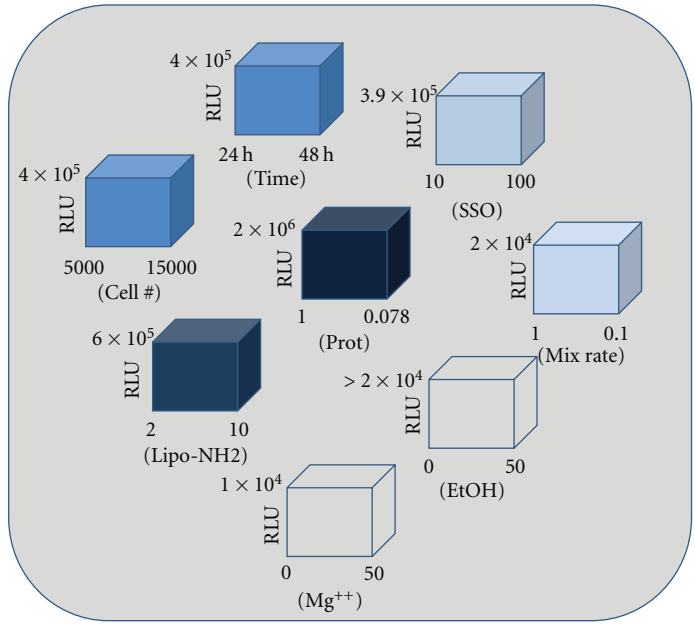

Figure 2: High-throughput screening experimental design analyzing parameters affecting SSO bioactivity in the Hela pLuc-705 system. RLU: relative luminescence, Lipo-NH2: lipofectamine, Prot: protamine concentration, ETOH: ethanol concentration, Mg^{++}: magnesium concentration.

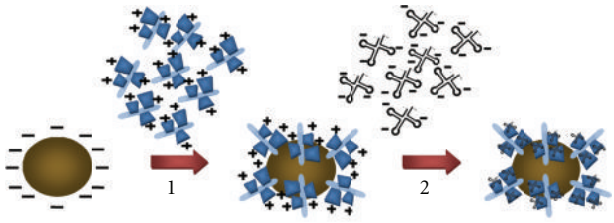

Figure 3: Hypothetical formation of biomolecular triconjugates of GNPs, protamine, and nucleic acid (figure not drawn to scale).

cells, suspended in 1X phenol red-free DMEM/10% FBS/1% penicillin and streptomycin, were seeded in 96-well plates in a volume of 100 μL per well. The cells were incubated at 37°C overnight, to allow them to attach. The DMEM was removed, and the cells were carefully washed with sterile 1X PBS. The GNPs and the conjugates, prepared as previously described, were centrifuged for 7 minutes at 15,000 rpm. The supernatant was removed, and the pellets were resuspended in serum-free, phenol red-free DMEM. From these solutions, 100 μL was added to each well, with 24 wells containing the GNPs and medium only, 24 wells containing the conjugates and medium, and 24 wells containing only the serum-free, phenol red-free medium. The plates were incubated overnight at 37°C. After incubation, the medium was removed and the cells were washed with sterile 1X PBS to remove any GNPs or conjugates, to avoid any interference with the absorbance readings. To each well, 100 μL of fresh serum-free, phenol red-free medium was added, along with 10 μL of a 12 mM MTT stock solution, prepared by adding 1 mL of sterile 1X PBS to 5 mg MTT (Invitrogen). The samples were mixed with the pipettes, and the plates were incubated for 4 hours at 37°C. All but 25 μL of the medium was removed, and 50 μL of DMSO was added to each well to solubilize the formazan. The solutions were mixed with the pipette, and allowed to incubate for 10 minutes at 37°C. The solutions were mixed again with the pipette, and the absorbance was read at 540 nm. This experiment was repeated three times, and the results are graphed in Figure 10.

3. Results and Discussion

3.1. Analysis and Sedimentation of Protamine : RNA. Direct NanoDrop measurement of protamine : RNA and microfuge sedimentation are shown in Figure 1. Macromolecule ($tRNA_{phe}$), rapidly mixed on a dual pump flow head with protamine, was sedimented at 13 k, and the supernatant and pellet or supernatant fractions tested on a NanoDrop UV/Vis instrument at 214, 260, 400, or 600 nm for peptide, RNA, or particle light scatter properties, respectively. The data demonstrate quantitative transferal of the protamine and RNA from the supernatant to the pellet. Light scatter of the particles formed is measured at 400 or 600 nm.

3.2. Measuring SSO Bioactivity in the HeLa pLuc-705 Model. We investigated the parameters that are important for SSO bioactivity in a high-low two-level experimental design. The experimental design and the data are shown in Figure 2. By looking at the relative luminescence (RLU), we conclude that the protamine concentration demonstrated the greatest positive outcome on splice-shifting activity whereas magnesium and ethanol concentration had a negative effect [15]. As shown in Figure 2, formulation-process variables were

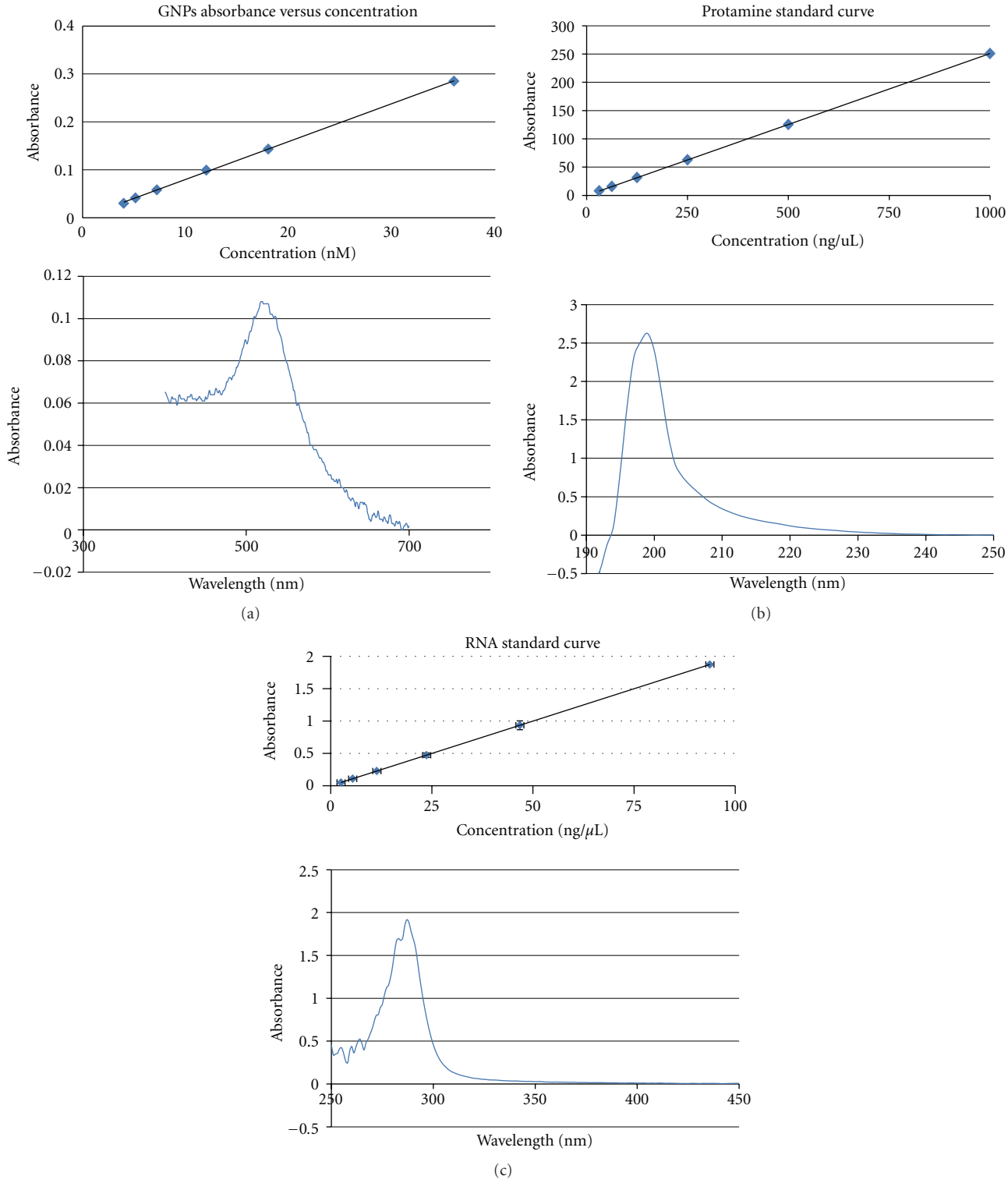

Figure 4: NanoDrop UV/Vis spectra (GNP, protamine, and RNA). Linear range in inset.

shown to affect the cells' luminescence by as much as 10^5–10^6 over background.

3.3. Au-Protamine : RNA Conjugates. GNPs are taken up by HeLa cells [13]. SSO delivery requires membrane penetration and nuclear localization, both of which are known capabilities of protamine [8]. Therefore, our next step was to create conjugates of GNP with protamine as illustrated in Figure 3. As diagrammed in Step 1, positively charged protamine molecules bind to the negatively charged gold nanoparticles

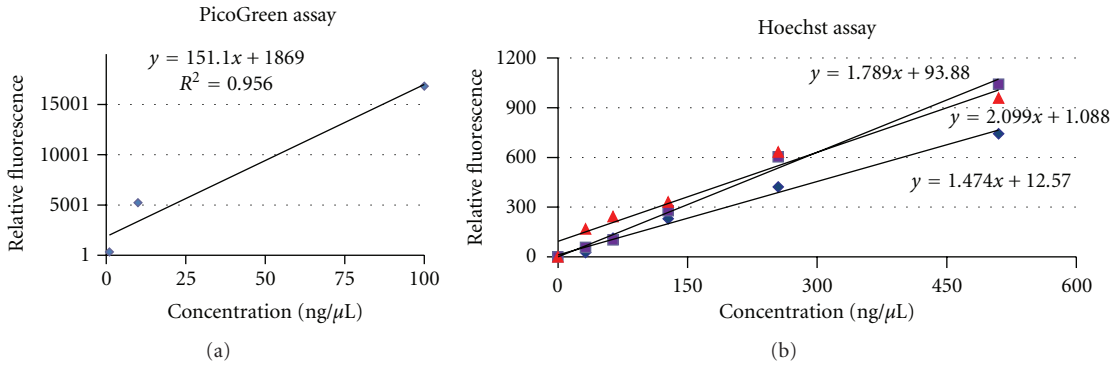

Figure 5: (a) PicoGreen and (b) Hoechst assays for dsDNA, demonstrating the increase in fluorescence as concentration increases in the ng/uL range.

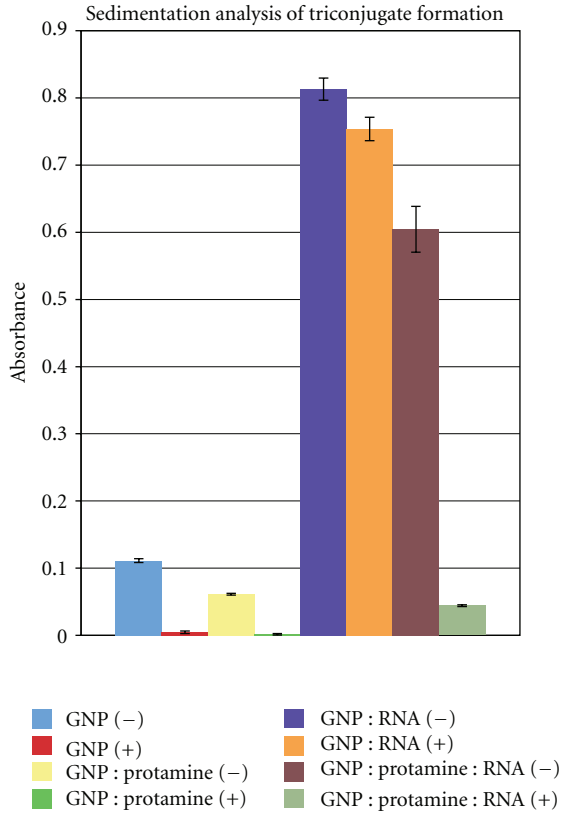

Figure 6: Loss of absorbance from the supernatant sedimentation analysis of GNP, GNP : protamine, GNP : RNA, or GNP : protamine : RNA; ± indicates before microcentrifuge spin (−) or after spin (+).

created by the citrate surface. In Step 2, negatively charged RNA molecules bind to the positively charged protamine molecules bound to a gold nanoparticle, completing the protamine/RNA/gold nanoparticle triconjugate.

3.4. Nano-Drop UV/Vis Analysis of the Nanoconjugate Components. The individual components of the triconjugates (e.g., GNP, protamine, or RNA) can be monitored by

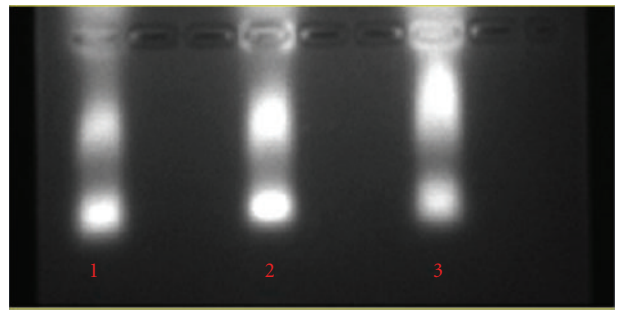

Figure 7: Agarose gel shift of RNA (lane 1), RNA + GNP (lane 2), or RNA + protamine + GNP (lane 3)).

NanoDrop UV/Vis (see Figure 4). Linear range of the standard curve is shown in the inset in units of nanograms per microliter or nanomolar. Maxima were RNA (260 nm), protamine (214–220 nm), and GNP (520–525 nm).

3.5. Fluorescence Analysis of DNA in the Nanorange. Double-stranded DNA (dsDNA) triconjugates with GNP and protamine can also be constructed. Concentration of dsDNA is obtained in the nanogram per microliter range by PicoGreen or Hoechst assays. Standard curves for dsDNA analysis, where fluorescence is a function of the DNA concentration, are shown in Figure 5.

3.6. Analysis of the Conjugates by Sedimentation. GNP, GNP-protamine, or GNP-protamine : RNA samples were analyzed on the UV/Vis NanoDrop before or after sedimentation on a microcentrifuge. The GNP in the supernatant was monitored at 525 nm and the RNA at 260 nm as described previously. These data are shown in Figure 6.

As can be seen in the figure, the greatest loss from the supernatant, based on the absorbance of the starting material, occurred for GNP-protamine : RNA triconjugate, thereby indicating the interaction of all three components.

3.7. Analysis of the Conjugates by Gel Shift. In a parallel experiment to that shown above in Figure 6, the GNP, GNP-RNA, or GNP-protamine : RNA were analyzed by agarose

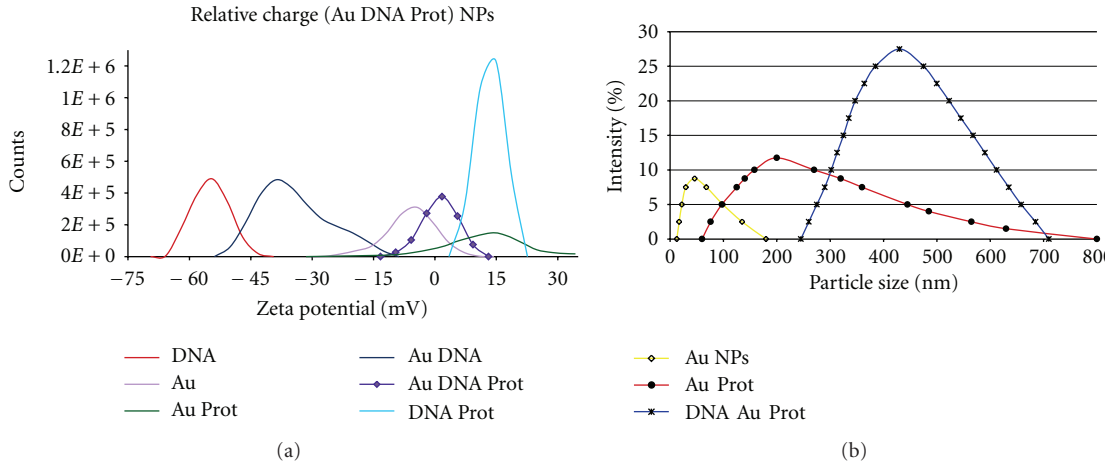

Figure 8: Evidence for bionanoconjugates made between GNPs, protamine, and DNA by DLLS analysis of (a) surface charge and (b) size distribution by intensity.

gel electrophoresis. These data are shown in Figure 7. A slight shift was observed upon interaction of RNA with GNP, and a more obvious shift occurred after the introduction of protamine, again suggesting the presence of the triconjugate species. Increased staining intensity in the well was observed previously for protamine : RNA nanoparticles [9].

3.8. Surface Charge and Size of the Conjugates. Zeta potential of the GNPs in the presence or absence of protamine and/or nucleic acid (DNA in this case) is shown in Figure 8(a). Potential of GNP alone was slightly less than zero. On the other hand, when protamine was added to either the GNPs or DNA, the zeta potential value increased to 12.5 mV and 13.4 mV, respectively, due to the positive charges on protamine. When all three were combined, the zeta potential value decreased to 1.20 mV, indicating a strong interaction.

Figure 8(b) shows the expected effect of conjugation on the particle's size. For the sample containing only the GNPs, the particle size is estimated to be approximately 38 nm. After complexing the GNP with protamine, as previously described, the particle size increases to approximately 200 nm. When the DNA is added, the sizes increases accordingly, to approximately 420 nm. This is further evidence that the conjugates are formed with all three components.

3.9. Spectral Shift upon Conjugate Formation. The GNP spectrum, shown in Figure 9, demonstrates the absorbance peak at approximately 520–530 nm, characteristic of particles in the low nanometer size range used here. The spectrum of the DNA displays the typical nucleic peak at 260 nm, which exhibits a greatly increased absorbance after interaction with protamine or protamine : gold. The mixture of DNA and protamine produced spectra that indicated strong interactions between the two molecules. The protamine : nucleic acid interaction is incompletely understood, and although the zeta potential data above suggest that the interaction is electrostatic in nature, the data also reveal an enhancement of absorbance for the DNA peak at 260 nm, thus implicating

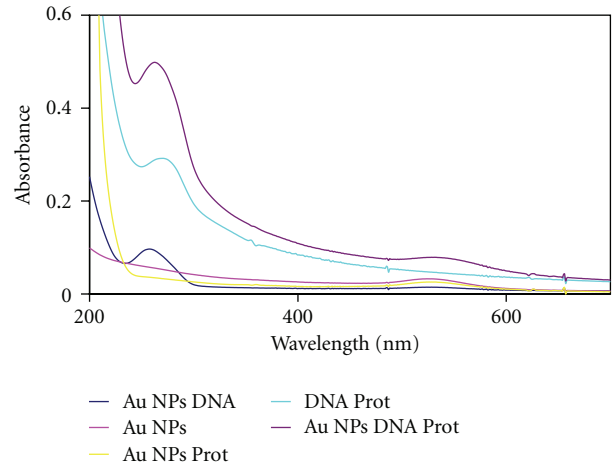

Figure 9: Evidence for bionanoconjugates made between GNPs, protamine, and DNA by UV/Vis.

some structural rearrangement. RNA : protamine and GNP-protamine : RNA were amplified and shifted further (data not shown).

3.10. Biocompatibility of Triconjugates. As previously reported, gold nanoparticles are taken up by HeLa cells [13]. The absorbance readings shown below, in Figure 10, confirm that the HeLa pLuc-705 cells retained their metabolic activity after the 24-hour incubation time with gold nanoparticles only, and with conjugates of gold nanoparticles, protamine, and RNA. This confirms that the conjugates are not cytotoxic, and this is a safe system for SSO delivery.

4. Conclusions

The high-low screening design experiment demonstrated that protamine, ethanol, and magnesium yielded the greatest influence on SSO bioactivity. The data, therefore, suggest

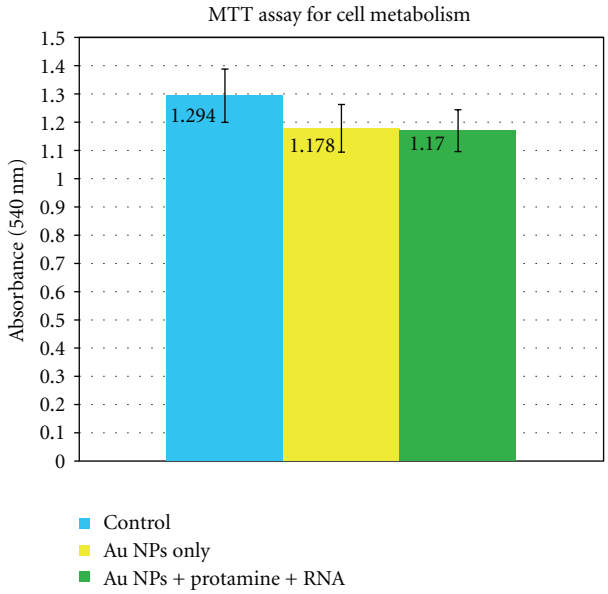

Figure 10: Evidence of continued cellular metabolic activity after incubation with triconjugates.

that creating conjugates in which protamine could affix RNA onto the GNP might be warranted. The data contraindicates condensing and/or precipitating protamine : RNA nanoparticles as a result of varying the ionicity and hydrophobicity [6, 15]. Modeling of protamine, based on dark field microscopy [16] and earlier studies [17, 18], suggests that protamine condenses DNA into nanoparticles, which here we hypothesize (Figure 3) can be extended to entrap RNA onto the protamine-GNP conjugates.

To understand the triconjugate of RNA, GNPs, and protamine by UV/Vis spectroscopy, it is first necessary to determine the spectrum of each component individually. Changes in the wavelength or peak amplitude after addition of a second and third component suggests their interaction whereas unchanged peaks indicate their dispersion. In erefFigurefig4, the individual peaks for nucleic acid, GNPs, and protamine are illustrated, which are compared subsequently to solutions of these components in combination, seen in Figure 9. Again, shifts in the amplitude or absorbance maximum in the RNA or gold UV/Vis spectra suggest triconjugate interaction between the three species: protamine, RNA, and GNP.

NanoDrop UV/Vis has nanorange sensitivity like its fluorescence counterparts, the PicoGreen and Hoechst assays, yet is not dependent on a double-stranded nucleic acid fordye binding. Although UV/Vis data suggests interaction between the triconjugates, at present it is uncertain that these fluorescent dyes can confirm this putative interaction; however, we did note a slight gel shift after staining with the fluorescent dye ethidium and consider this observation to be consistent with interactions between GNP, protamine, and RNA.

The NanoDrop instrument can rapidly quantify nucleic acids, protamine, or gold conjugates in UV or visible mode in the nanomolar or nanogram per microliter range, although its utility in evaluating breakdown products or biomaterial and nanomaterial compatibility with proteins and nucleic acids remains in question. For on-particle analysis, however, DLLS and NanoDrop UV/Vis observations are critical for optimizing preparation and delivery.

There is substantial interest in the formulation and delivery of therapeutic nucleic acids as nanoparticles for delivery in humans [1]. Here, methods amenable for the analysis of macromolecular RNA and DNA, and those present as nanoparticles, have been compared. DLLS, fluorimetric, UV/Vis spectroscopic, and electrophoretic methods are all capable of nanorange detection. Accordingly, these assays are likely to have mainstay applications in the clinical progression of delivering nucleic acids into patients in the form of nanoparticles.

Acknowledgments

The authors would like to thank their collaborators, particularly Drs. Lifeng Dong, Michael Craig, Richard Garrad, and Garry Glaspell for their generous support, encouragement, and helpful discussions. R. K. DeLong, K. Ghosh, and A. Wanekaya are supported by an AREA/R15 Grant from the National Cancer Institute titled, "Anti-Cancer RNA Nanoconjugates" (1 R15 CA139390-01).

References

[1] M. Davis, J. Zuckerman, C. Choi et al., "Evidence of RNAi in humans from systemically administered siRNA via targeted nanoparticles," *Nature*, vol. 464, no. 7291, pp. 1067–1070, 2010.

[2] J. A. Bauman, S. D. Li, A. Yang, L. Huang, and R. Kole, "Anti-tumor activity of splice-switching oligonucleotides," *Nucleic Acids Research*, vol. 38, no. 22, pp. 8348–8356, 2010.

[3] M. A. Garcia-Blanco, "Alternative splicing: therapeutic target and tool," *Progress in Molecular and Subcellular Biology*, vol. 44, pp. 47–64, 2006.

[4] E. Collins, J. C. Birchall, J. L. Williams, and M. Gumbleton, "Nuclear localisation and pDNA condensation in non-viral gene delivery," *Journal of Gene Medicine*, vol. 9, no. 4, pp. 265–274, 2007.

[5] L. Benimetskaya, N. Guzzo-Pernell, S. T. Liu, J. C. Lai, P. Miller, and C. A. Stein, "Protamine-fragment peptides fused to an SV40 nuclear localization signal deliver oligonucleotides that produce antisense effects in prostate and bladder carcinoma cells," *Bioconjugate Chemistry*, vol. 13, no. 2, pp. 177–187, 2002.

[6] B. Scheel, R. Teufel, J. Probst et al., "Toll-like receptor-dependent activation of several human blood cell types by protamine-condensed mRNA," *European Journal of Immunology*, vol. 35, no. 5, pp. 1557–1566, 2005.

[7] L. Li, S. A. Pabit, S. P. Meisburger, and L. Pollack, "Double-stranded RNA resists condensation," *Physical Review Letters*, vol. 106, no. 10, article 108101, 2011.

[8] F. Reynolds, R. Weissleder, and L. Josephson, "Protamine as an efficient membrane-translocating peptide," *Bioconjugate Chemistry*, vol. 16, no. 5, pp. 1240–1245, 2005.

[9] R. K. DeLong, U. Akhtar, M. Sallee et al., "Characterization and performance of nucleic acid nanoparticles combined with protamine and gold," *Biomaterials*, vol. 30, no. 32, pp. 6451–6459, 2009.

[10] O. Nakagawa, X. Ming, L. Huang, and R. L. Juliano, "Targeted intracellular delivery of antisense oligonucleotides via conjugation with small-molecule ligands," *Journal of the American Chemical Society*, vol. 132, no. 26, pp. 8848–8849, 2010.

[11] S. Resina, R. Kole, A. Travo, B. Lebleu, and A. R. Thierry, "Switching on transgene expression by correcting aberrant splicing using multi-targeting steric-blocking oligonucleotides," *Journal of Gene Medicine*, vol. 9, no. 6, pp. 498–510, 2007.

[12] S. H. Kang, M. J. Cho, and R. Kole, "Up-regulation of luciferase gene expression with antisense oligonucleotides: implications and applications in functional assay development," *Biochemistry*, vol. 37, no. 18, pp. 6235–6239, 1998.

[13] B. D. Chithrani, A. A. Ghazani, and W. C. Chan, "Determining the size and shape dependence of gold nanoparticle uptake into mammalian cells," *Nano Letters*, vol. 6, no. 4, pp. 662–668, 2006.

[14] R. R. Arvizo, O. R. Miranda, M. A. Thompson et al., "Effect of nanoparticle surface charge at the plasma membrane and beyond," *Nano Letters*, vol. 10, no. 7, pp. 2543–2548, 2010.

[15] Z. Reich, R. Ghirlando, and A. Minsky, "Secondary conformational polymorphism of nucleic acids as a possible functional link between cellular parameters and DNA packaging processes," *Biochemistry*, vol. 30, no. 31, pp. 7828–7836, 1991.

[16] F. P. Ottensmeyer, R. F. Whiting, and A. P. Korn, "Three dimensional structure of herring sperm protamine Y-I with the aid of dark field electron microscopy," *Proceedings of the National Academy of Sciences of the United States of America*, vol. 72, no. 12, pp. 4953–4955, 1975.

[17] Z. Lin, C. Wang, X. Feng, M. Liu, J. Li, and C. Bai, "The observation of the local ordering characteristics of spermidine-condensed DNA: atomic force microscopy and polarizing microscopy studies," *Nucleic Acids Research*, vol. 26, no. 13, pp. 3228–3234, 1998.

[18] L. R. Brewer, M. Corzett, and R. Balhorn, "Protamine-induced condensation and decondensation of the same DNA molecule," *Science*, vol. 286, no. 5437, pp. 120–123, 1999.